LANGMUIR

Subscriber access provided by University of Portsmouth

Article

Polymer-lipid microparticles for pulmonary delivery

Georgios K. Eleftheriadis, Melpomeni Akrivou, Nikolaos Bouropoulos, John Tsibouklis, Ioannis S Vizirianakis, and Dimitrios G. Fatouros

Langmuir, **Just Accepted Manuscript** • DOI: 10.1021/acs.langmuir.7b03645 • Publication Date (Web): 27 Feb 2018

Polymer-lipid microparticles for pulmonary delivery

Georgios K. Eleftheriadis,[±] *Melpomeni Akrivou,*[#] *Nikolaos Bouropoulos,*[¶,¦] *John Tsibouklis,*[§] *Ioannis S. Vizirianakis,*[#] *Dimitrios G. Fatouros* [±,*]

[±]Laboratory of Pharmaceutical Technology, School of Pharmacy, Aristotle University of Thessaloniki GR, 54124

[#]Laboratory of Pharmacology, School of Pharmacy, Aristotle University of Thessaloniki GR, 54124

[¦]Department of Materials Science, University of Patras, 26504 Rio, Patras, Greece

[¶]Foundation for Research and Technology Hellas, Institute of Chemical Engineering and High Temperature Chemical Processes, Patras, Greece

[§]School of Pharmacy and Biomedical Sciences, University of Portsmouth

ABSTRACT

Towards engineering approaches that are designed to optimize the particle size, morphology and mucoadhesion behavior of the particulate component of inhaler formulations, this paper presents the preparation, physicochemical characterization and preliminary *in vitro* evaluation of multicomponent polymer-lipid systems that are based on "spray-drying engineered" α-lactose monohydrate microparticles. The formulations combine an active (budesonide) with a lung surfactant (dipalmitoylphosphatidylcholine) and with materials that are known for their desirable effects on morphology (polyvinyl-alcohol), aerosolization (L-leucine) and mucoadhesion (chitosan). The effect of the composition of formulations on the morphology, distribution and *in vitro* mucoadhesion profiles is presented along with "Calu-3 cell monolayers" data that indicate good cytocompatibility and also with simulated-lung-fluid data that are consistent with the therapeutically useful release of budesonide.

Keywords: *engineered microparticles, mucoadhesion, cytocompatibility, pulmonary delivery.*

INTRODUCTION

Elevated blood flow and a large surface area (100 m^2) render the human lung network a suitable site for the rapid absorption of therapeutic compounds.[1] The pulmonary delivery of drugs by means of inhaled aerosols is regarded as a minimally invasive route of administration and offers the additional advantages that are associated with the avoidance of the hepatic first-pass effect. The benefits of the approach are counterbalanced by the challenges associated with the efficient delivery of therapeutic formulations to the lungs, which is often impeded by physiological barriers that inhibit the efficient deposition, residence time and drug release characteristics of formulations. For effective delivery of therapeutic compounds to the alveolar area of the lungs, it is desirable that solid components of inhalable formulations have a mean aerodynamic diameter in the range 1-5 μm.[2] Associated with this are the good aerosolization properties of particles, such that aggregation is prevented.[3] Also, to overcome the action of the mucociliary apparatus,[4,5] the particles must be mucoadhesive, such as to become instantaneously integrated into the mucosa layer of the lungs. To this end, many excipients (sugars,[6,7] lipids,[8,9] amino acids,[10,11] polymers[12,13]) have been evaluated[14] but lactose has remained the material of choice for commercial formulations over many years.[15]

The method of choice for the manufacturing of both local and systemic formulations for the delivery of therapeutic agents to the respiratory system is spray drying.[3,16,17] Within the context of particle engineering, spray drying is an established method for the formulation of drug-loaded particles since it is compatible a wide range of materials[18] and offers the capability to fine-tune multicomponent formulations through the incorporation of an array of well-studied excipients in a one-step method that allows the ready incorporation of therapeutic compounds.[19–22]

This paper describes the engineering, by spray drying, of multicomponent formulations for the pulmonary delivery of the corticosteroid budesonide (BD), which is widely used for the treatment of asthma. In accord with established technologies, the bulk material of the formulation is α-lactose monohydrate (LCS). The other components of the formulation include: polyvinyl alcohol (PVA), which is reported to enhance the morphological characteristics of particles and to improve their drug-release properties;[23–25] dipalmitoylphosphatidylcholine (DPPC) lung surfactant;[26–29] L-leucine (L-LC) aerolization modifier;[25,30,31] and chitosan (CS) bioadhesive.[32–35] To facilitate the selection of optimal compositions, these formulations are assessed for their production yield, morphological characteristics, and surface charge. Thermal analysis and infrared spectroscopy are used to further characterize promising formulations, and these studies are complemented by laser diffraction investigations of particle size distribution and aerolization performance, and also by *in vitro* deposition studies. The *in vitro* release of the incorporated active is assessed in simulated lung fluid. To simulate the *in vivo* challenges that are presented to the formulations by the mucosal barrier at the surfaces of the lung, assessment tools are deployed for the evaluation of the mucoadhesive properties of the microparticles under investigation. Both the adhesion profiles of microparticles in contact with mucus and the effects of this interaction on the cohesiveness of the resultant gel are considered for the purpose of identifying a potentially therapeutically useful formulation. Finally, cell proliferation and epithelial integrity studies are used to evaluate the effect of formulations on the Calu-3 cell line.

EXPERIMENTAL SECTION

Materials. Budesonide (≥99%), polyvinyl alcohol (Mowiol 4-88, MW~31000), L-leucine (≥98%), low molecular weight chitosan (MW 50000-190000), Rhodamine B (≥95%), diethylenetriaminepentaacetic acid (≥99%), RPMI 1640 amino acids solution, deoxyribonucleic acid sodium salt from salmon testes, mucin from porcine stomach type II and gelatin from bovine skin type B were all purchased from Sigma-Aldrich, Germany. α-Lactose monohydrate was purchased from DMV International, Netherlands. Egg Yolk Emulsion for Microbiology was sourced from Merck, Germany. 1,2-Dipalmitoyl-*sn*-glycero-3-phosphocholine (DPPC) was obtained from Avanti Polar Lipids. All other materials and reagents were of analytical grade.

Homogenised Mucus. An aqueous mixture was prepared from sodium chloride (0.9% w/v), the bacteriostatic agent sodium azide (0.02% w/v), the oxidation-inhibiting chelating agent ethylenediaminetetraacetic acid (0.186% w/v) and an ethanolic solution (1ml) of the protease (cell-degradation) inhibitor phenylmethylsulphonyl fluoride (0.0175% w/v). The mixture was made up to 100ml with distilled water and brought into the solution phase by stirring (12 hours, room temperature). In accord with the procedures dictated by the Science Faculty Ethics Committee of the University of Portsmouth, crude sputum (100 ml) was collected from two unfed (3 hours) healthy human volunteers (one male, one female; both 24 years of age) over a period of approximately 3 hours (The average daily flow of whole saliva in healthy subjects varies between 1 and 1.5 L[36]) and subjected to vacuum (Buchner) filtration (twice) to remove any buccal cells, food debris and other large particles. The thus treated mucus was preserved by freezing at -18ºC.

Preparation of engineered microparticles. Three sets of multicomponent carriers (MCs) were produced by the spray drying technique, namely: budesonide-free (empty), budesonide-loaded

and Rhodamine B-loaded microparticles. For each set, the effect of variations in the proportions of excipients was assessed at two specified ratios of the utilized liquid media (water and ethanol). The compositions of empty formulations are listed at Table 1. The excipients PVA, LCS, DPPC, CS and L-LC were incorporated into the formulation from feed solutions. To prepare each formulation, the lipid DPPC was dissolved in a specified volume (70 or 85 mL) of ethanol. In parallel, PVA was dissolved in a predetermined amount of hot (90 ºC) water (either 25 or 10mL), and once PVA had dissolved, LCS and L-LC were added in sequence to each solution. Separately, CS was dissolved in water containing 1% acetic acid (5 mL). The two aqueous solutions were mixed to form the aqueous phase, which in turn was added very slowly to the organic phase – such as to avoid the precipitation of the lipid compound or the formation of liposomal structures. The mixing of the alcoholic and aqueous solution was in such ratios as to afford formulations that had a total volume of 100 mL and a solid content of 0.1% w/v.

To prepare loaded formulations, selected compositions of empty feed solutions were prepared from budesonide (BD) and budesonide plus Rhodamine B (RH) feed solutions at 5% w/w (5 mg BD or BD+RH per 100 mg of total solids). In both cases, BD and RH were respectively added to the ethanolic and aqueous solutions while the lactose content was reduced by an equal (weight) amount, such as to maintain the total solid content of the final feed solution at 0.1% w/v. To limit the effect of evaporation on the total volume of the liquid media, the feed solutions were subjected to gentle stirring (5 min) at 50 ºC; the boiling points of H_2O:EtOH at 30:70 v/v is at 85 ºC while that at 15:85 v/v is 80 ºC.[37] The feed solutions were spray dried using a Buchi Mini Spray Dryer B-191 (Buchi, Switzerland) operating at: inlet temperature, 100 ºC; airflow, 600 L/h; respective aspirator and pump rates of 100 % and 4.5 mL/min; and, outlet temperature of 60-65 ºC. To calculate the yield of the spray-drying process, each batch of MCs was weighed and

the percentage yield was determined from: $Yield\%=m_f/m_i\times100$; where m_i is the initial mass of solids in feed solutions and m_f is the collected mass of MCs. To quantify drug loading, an accurately weighed amount of *ca*. 2 mg of each sample was added to EtOH (5 mL). This mixture was stirred continuously for 24 h before the solid content was separated by centrifugation (4000 rcf, 15 min). The drug content in the supernatant was determined by HPLC and percentage loading was calculated from: $DrugLoad\%=m_{BD}/m_{BD\text{-}MC}\times100$, where m_{BD} is the determined mass of budesonide and $m_{BD\text{-}MC}$ is the mass of drug loaded MCs dispersed in EtOH. In a similar manner, the drug loading of RH in the carriers was quantified spectrofluorimetrically following dissolution of the dye-containing carrier (3 mg) in EtOH (10 mL). Microparticles were stored in a $CaCl_2$ desiccator.

Scanning electron microscopy and ζ-potential studies. To assess particle morphology, both empty and loaded microparticles were visualized using a Zeiss SUPRA 35VP SEM microscope. Dispersion stability studies were performed by means of a Zetasizer Nanoseries Nano-ZS analyzer (Malvern, UK). Microparticles were dispersed in distilled water (0.2 mg/mL), sonicated (15 s), and ζ-potential determinations were performed in triplicate.

Infrared spectroscopy and thermal analysis. The infrared spectra (650-4000 cm^{-1}, 2 cm^{-1} resolution) of loaded formulations and of each of their constituents were obtained using an IR Prestige-21 (Shimadzu, Japan) instrument. Differential Thermal analyses (5mg, aluminum pans, 20-350 ºC, 10 ºC /min) of selected empty, loaded and pristine materials were performed using a DSC 204 F1 Phoenix (Netzsch) instrument.

Laser diffraction analysis. Laser diffraction (Malvern Spraytec; Malvern, UK) studies allowed the evaluation of the particle size distribution (PSD) of loaded carriers: Gelatin capsules were filled with approximately 15 mg of the formulation under study, and these powders were

delivered by attaching a breath-activated spray delivery device to a USP throat that had been mounted onto the Spraytec device. A 300 mm focal length lens (specified for the particle size range 0.1-900 μm) was used and the respective refractive indices for particles and dispersant (air) were set at 1.330 ± 0.001 and 1.000 ± 0.001. Light scattering patterns were recorded in triplicate at the flow rate of 30 L/min and the volumetric percentiles $D_v(10)$, $D_v(50)$, $D_v(90)$: the percentage of particles with geometric diameter < 5μm and the span of the distribution was recorded.

***In vitro* aerosolization and deposition**. The aerodynamic performance of Rhodamine-loaded microparticle formulations was evaluated by the PSD analysis of data obtained using an Andersen Cascade Impactor (ACI) in a configuration that had been designed to simulate the deposition of particles on the respiratory tract. To this end, an accurately weighed amount (*ca*. 60 mg) of Rhodamine-loaded MCs was divided equally amongst three gelatin capsules. The device was allowed to equilibrate to steady flow (30 L/min for 10 min), after which time the Rhodamine-loaded MCs were introduced in the ACI over 15 sec at the same air flow rate. The air flow was then interrupted, and the device was allowed to equilibrate for an additional period of 2 min. The ACI stages were disassembled, rinsed (ethanol) and the deposited MCs at each stage were collected in separate glass vials. To facilitate the solubilization of RH, each of these ethanolic solutions was kept under stirring for 2 h (room temperature). To separate the insoluble mass, aliquots of each solution were centrifuged at 4000 rcf for 20 min, and the amount of RH deposited in each stage was quantified by spectrofluorimetry measurements (RF-5301-PC Fluorescence Spectrophotometer, Shimadzu): excitation (570 nm) and emission (590 nm) at respective slit widths of 3 and 5 nm. The calibration curve of Rhodamine was linear over the range of 0.01-0.05 μg/mL ($R^2 \geq 0.999$). Data for the % cumulative RH mass that had been

adjusted for the stated aerodynamic diameter were plotted, on a semi-log, as a function of the respective aerodynamic diameter, according to Ph.Eur. The fine particle fraction (FPF) was derived at 5 μm cut-off diameter and the mass-median aerodynamic diameter (MMAD) was determined at 50% cumulative mass. The geometric standard deviation (GSD) was calculated from $GSD=(AD_{84.13}/AD_{15.87})^{1/2}$, where $AD_{84.13}$ and $AD_{15.87}$ are the aerodynamic diameters representing cumulative masses of 84.13% and 15.87%, respectively.

The behavior of microparticles in artificial mucus. The behavior of empty and RH- loaded MCs was investigated by ζ-potential measurements and by permeation studies, respectively in mucin dispersion and in artificial mucus.[38] ζ-Potentials of empty formulations were recorded in mixtures with mucin dispersion (0.02% w/v).

In an effort to assess the capability of RH-loaded microparticles to penetrate the mucus layer of the respiratory system, preliminary permeation studies were conducted by means of an established *in vitro* model. [38] (The adopted model is not capable of simulating the *in vivo* conditions; it is a tool for the pre-screening of the capability of carriers to participate in mucoadhesive interactions.) This barrier was simulated by a layer of gelatin that had been placed at the bottom of a test tube and covered with artificial mucus consisting of an aqueous dispersion of DNA, mucin, sterile egg yolk emulsion, diethylenetriaminepentacetic acid, sodium chloride, potassium chloride and RPMI medium. A specified volume of an aqueous dispersion of microparticles was placed on the artificial mucus layer. The test tubes were kept at room temperature for 24 h, after which time the amount of Rhodamine that had penetrated the mucus and became deposited on the gelatin layer was quantified by fluorimetry. Experiments were conducted in triplicate.

To further assess the mucoadhesive properties of the BD loaded formulations, a Stable Micro System (TA.XT.plus) Texture Analyser was employed to record their combined adhesion-cohesion profiles following integration into homogenized mucus. Onto the probe was attached, by means of double-sided adhesive tape, an accurately weighted amount (*ca*. 5 mg) of the sample under test, while onto the holder stage of the device was deposited homogenised mucus (*ca*. 0.25 mL). The probe moved downward to establish contact with the mucus layer before being withdrawn at a specified constant rate. The experiments were performed under a force of 5 g, a contact time of 10 s and probe speed of 1 mm/sec. The mucoadhesion profiles were recorded as plots of force *versus* time.

***In vitro* release in Simulated Lung Fluid.** Release studies were carried out in simulated lung fluid (SLF).[39,40] Each BD loaded sample (8 mg) was separately suspended in SLF (4 mL) that had been maintained at 37 ºC. Dialysis bags (12,000 - 14,000 molecular weight cut-off) were filled with each suspension (1 mL) and immediately immersed in an SLF-containing (20 mL) glass vial maintained at 37 ºC. Drug release was carried out over 24 h in a shaking thermostatic (37 ºC) water bath. At predetermined time intervals (0, 5, 10, 20, 30, 60, 90, 120, 180, 240, 300, 360, 720 and 1440 min), aliquots of 1 mL of the release medium were withdrawn, and instantly replaced with fresh SLF. The concentration of BD in each aliquot was determined using an HPLC system consisting of an LC-10 AD VP pump, a SIL-20A HT autosampler and a UV-Vis SPD-10A VP detector that had been interfaced to Class VP Chromatography data system v.4.3 (Shimadzu):[41] stationary phase, Ascentis C8 column (150 mm, 4.6 mm, 5μm); mobile phase, acetonitrile potassium dihydrogen phosphate (60:40 v/v; 0.025M; pH 3.2, adjusted with phosphoric acid). The mobile phase was degassed (sonication, 20 min) before each measurement. The flow rate and injection volume were 1.1 mL/min and 10 μL, respectively. The

detection of BD (retention time, 4.6 min) was at 244 nm. The sample run time was 6 min. The calibration curve of budesonide was seen to be linear over the of range 0.1-0.6 μg/mL ($R^2 \geq 0.999$).

Calu-3 cell studies. The Calu-3, human adenocarcinoma-derived cell line, was used throughout the course of this study, from passages 25-33 in the transport experiments. Calu-3 cell cultures were grown in 75 cm^2 flasks (Corning Costar Corp., USA) in DMEM/F12 (Invitrogen Gibco, USA) medium that had been supplemented with 10% v/v Fetal bovine serum (FBS) and 100 μg/mL of penicillin/streptomycin and allowed to grow to 70-80% confluency. These were transferred in Transwell inserts (0.4 μm pore size, Corning Costar Corp., USA) at a density of 5 x 10^5 cells per well, and the cells were permitted to proliferate (37 ºC) in a humidified atmosphere containing 5% v/v CO_2. The cells were allowed to grow (Transwell inserts, 48 h) under liquid culture conditions (LCC), after which time the medium of the apical side was removed – thus allowing these cells to grow at the air interface environment (AIC). Every 48 h, the culture medium on the basolateral side was replaced and the integrity of the Calu-3 monolayer was ascertained by monitoring the transepithelial electrical resistance (TEER). Measurements were carried out using a Millicell ERS Voltohmmeter (EMD Millipore) equipped with chopstick electrodes. The daily monitoring of TEER values of monolayers allowed the selection of those giving readings >180 $\Omega*cm^2$. The measured TEER values were expressed as the percentage of those for control (untreated) cultures. To assess cell monolayer integrity and permeability, the TEER of Calu-3 monolayers that had been incubated with test formulations (1 mg/mL) was monitored at 60 min intervals over 240 min (Millicell-ERS; Millipore, Bedford, MA). The capability of the such treated monolayers to recover from the effects of the treatment

was assessed by washing the cell cultures with DMEM (to remove the formulations), before fresh HBSS/HEPES buffer was added and the TEER being monitored for a further 240 min.

Cytotoxicity assays. The cellular proliferation capacity of Calu-3 cells was assessed by exposing cultures to specified concentrations of the microparticles under test. Calu-3 cells were seeded at a density of 10^5 cells per well in 24-well culture plates (Corning Costar Corp., USA) and allowed to grow for a period of 48 h. Cells were then washed with PBS (pH 7.4) and the medium was replaced with 1 mL of FBS-free medium containing varying concentrations of the agents under investigation. The cell growth was measured by counting the number of cells in culture, using a hemocytometer. The viability of Calu-3 cells was assessed using the Trypan Blue method.[42]

Statistical analysis. All measurements are presented as mean ± SD. Values of $P<0.05$ are considered to denote statistical significance (Student's t-test).

RESULTS AND DISCUSSION

Evaluation of engineered microparticles. The solid composition of empty feed solutions, the calculated process yields and the ζ-potential values of empty MCs are presented at Table 1. Irrespective of variations in the proportion of excipients, in most cases, the spray drying process was associated with yields in the range 28 - 32%. Indicative of the role of PVA as the core material of formulations, S1 was produced at a low yield. In light of literature reports,[43] it is assumed that the yield of the process.is markedly influenced by the proportion of DPPC in the S1 formulation (S1 has the highest content of DPPC among all formulations under consideration).

In the processing of samples with the same composition (S3-S7 and S5-S6), the proportion of EtOH in the H_2O:EtOH medium (30:70 or 15:85) had a negligible effect ($P>0.05$) on the yield of the process if all other process parameters remained unaltered; indicating that the lower boiling

point of the more ethanolic medium does not accelerate the drying process, presumably due to molecular-level solvent association phenomena.

The surface charge studies reflected the strong dispersion stability of the empty particles in H_2O, with positive ζ-potential values in the range of 28.7-51.4 mV originating from the positive charge of CS[44] and also from the zwitterionic nature of the DPPC molecule which favours positive charges in the moderately acidic aqueous environment.[45] The influence of DPPC content on the ζ-potential was investigated in formulations having a fixed proportion of chitosan. Marked differences were noted between samples of low and high DPPC content. Indicative of plateau effects, however, S1 (40% DPPC) was characterized by a very similar ζ-potential to S5 (30% DPPC): respectively 29.3 ± 1.7 mV and 28.7 ± 1.5 mV. The corresponding differences between S2 (20% DPPC) and S3 (15% DPPC) were somewhat more pronounced at 40.8 ± 0.9 mV and 37.5 ± 0.6 mV, respectively. It is possible that the indicated increases in surface charge with increasing proportions of the nonionic core excipients, PVA and LCS, reflect the migration of the positively charged CS and DPPC molecules to the outer layer of particles. Amongst the empty MCs, the highest ζ-potential (51.4 mV) was associated with S4, which was formulated with triple the amount of CS (6% vs. 2%).

The size and morphological features of empty MCs were assessed by SEM imaging. Large particles (>>5 μm) were observed with S1 and S2 (Supplementary information, Figure S1). The SEM observations showed that other desiccated particles were approximately spherical and had smooth surfaces, and that their sizes were in the therapeutically useful range of 0.5-5.0 μm, Figure 1 (A, B, and C). The combined evaluations of experimental findings from the spray drying process, ζ-potential measurements and SEM imaging, allowed the selection of three candidate formulations for loading with BD and RH, namely: S3, S4 and S6.

Loaded formulations were prepared in an identical fashion to their free congeners by substituting 5% w/w of BD or RH for an equal proportion of LCS, such as to maintain a constant total content of solids at 0.1% w/v, Table 2. The incorporation in the formulation of the drug or the fluorescent molecule did not affect significantly the yields of formulations as compared with those associated with their empty counterparts ($p>0.05$): 29.2-33.8% and 31.1-34.6% respectively for budesonide and Rhodamine-loaded microparticles. Similarly, SEM micrographs revealed that budesonide did not effect any significant changes to morphology, Figure 1 (D, E, and F).

FTIR and DSC analysis. The FTIR spectra of pure BD, of each excipient and of drug loaded samples are presented in Figure 2. Pure budesonide exhibits characteristic bands at 3491 cm^{-1} (OH stretch), 2947 cm^{-1} (CH_2 stretch), 1718 cm^{-1} and 1664 cm^{-1} (C=O stretches) and 1624 cm^{-1} (C=C).[46,47] None of these features were indisputably visible in the spectra of loaded formulations (owing to the masking effect of the DPPC component, which is characterized by a broad OH stretch (3150cm^{-1} - 3550cm^{-1}) and absorptions at 2916 cm^{-1}, 2848 cm^{-1} and 1732 cm^{-1}, respectively due to CH_2 asymmetrical and symmetrical stretches and the C=O stretching vibration[48]). The dominance of DPPC is demonstrated by the intensity of BD1 bands (30% w/w DPPC) as compared with those of BD2 or BD3 (15% w/w DPPC).

DSC traces of constituents and formulations are presented in Figure 3. The thermogram of DPPC exhibits a broad endotherm in the range of 38-54 ºC, which is assumed to mark the transition from gel to a lipid-crystalline state. The melting endotherm of PVA was observed at 193 ºC, while evidence for the oxidative degradation of this polymer is provided by a peak that is centered at *ca*. 325 ºC. CS presented a dehydration endotherm that was centered at *ca*. 104 ºC, and an exothermic decomposition that is onset at *ca*. 280 ºC. The thermograms of LCS, pure BD

and L-LC indicated the melting temperatures of these components at 240 ºC, 260 ºC and 320 ºC, respectively. The thermograms of BD formulations were marked by endothermic phenomena over the temperature range 230-320 ºC. As compared with the DSC traces characterizing the base component of the macroparticulate formulation, there is observed a shift in the positions of the observed transitions of formulations towards higher or lower temperatures that is notably dependent upon the relative ratios of LCS, BD and L-LC. Since spay-dried LCS is well known to exist in the amorphous state but to become progressively crystalline over time,[49] it is assumed that it is the influence of the proportion of the other components of the formulation that determines the rate of the crystallisation process and hence the thermal behavior of the formulation. BD3, which has the maximum content of LCS and minimum content of L-LC, exhibits a melting endothermic which is centered at 276 ºC while for BD2 the same transition is at 278 ºC. Indicative of phase separation, BD1 exhibits a two-stage melting process with a distinct inflexion at 270 ^{o}C and a shoulder at 287 ^{o}C. Accordingly, it is assumed that BD1 behaves as a multicomponent system of its constituent molecules and that L-LC, BD and LCS are key to the intimate mixing of the constituent molecules at the molecular level; as is the case with BD2 and BD3. Comparative studies involving the empty formulations show heat capacity minima at 277 ºC and 275 ºC respectively for S4 and S3, which are consistent with those observed with the corresponding loaded formulations BD2 and BD3. S6 exhibits distinct minima at 269 ºC and at 287 ºC, which show that the replacement of the BD content by an equal amount of LCS effects a slight shift (1 ºC) in the minima towards lower temperatures. The higher-temperature melting endotherms of BD formulations as compared with those of their S counterparts is consistent with successful loading.

Particle size distribution and *in vitro* deposition. Particle sizes of loaded formulations, as determined by laser diffraction, are presented in Table 3. The volumetric median diameter of the samples, which is related to the geometric diameter, was in the range 8.98-9.74 μm ($P<0.05$), while the percentage of particles with size <5μm was about 20% for BD1 and 23% for BD3; representative size distribution plots are presented in Figure 4A-C. In accord with SEM data, BD3, which has the highest content of PVA and LCS, is confirmed as the formulation that exhibits the most useful, for the proposed use, size distribution profile. By contrast, the size distribution profile of BD1, which has the lowest PVA and LCS contents, was sensitive to increases in the volumetric percentiles and to the volumetric fine particle fraction. Data for BD2 (volumetric median diameter, 9.29 μm; 21.96% particles <5 μm) confirm the aerosolization effect of L-LC[31,50] (*c.f.* BD1). Large particles were formed in BD formulations, and these are reflected in incremented $D_v(90)$ values of 26.43 μm, 26.84 μm and 30.33 μm, respectively for BD2, BD3 and BD1. The size plots of the drug loaded formulations revealed unimodal distributions with spans in the range 2.30-2.75 μm.

The particle size analysis was complemented by *in vitro* deposition studies of Rhodamine-loaded formulations using the multistage-ACI. The Rhodamine formulations were prepared under identical condition to those used for the drug-loaded samples, such that they provide a fluorescently labelled congener of the therapeutically useful formulation, which can be used to compare size distribution data from laser diffraction experiments and the ACI-mediated aerosolization studies.

The deposition of the RH-loaded MCs onto the stages of the ACI is illustrated at Figure S2 (Supplementary Information). The deposited particles were seen to form as spots that were distributed over the surface of each level. This is attributed to capillary air flow at the lower

stages of the ACI device. The particle size distributions and the calculated MMAD, GSD and FPF values of Rhodamine microparticles are presented in Figure 4D and summarized in Table 3. Consistent with expectation on the basis of PVA-LCS content, *ca*. 65% of particles RH3 presented an aerodynamic diameter <5 μm and a mean diameter of *ca*. 4 μm. In accord with expectation, the low PVA and LCS-content formulations RH1 and RH2 were characterized by aerodynamic diameters of *ca*. 6 μm and respective FPFs of 23% and 38%. Since the PVA and LCS content of RH1 and RH2 is almost identical, the marked differences in behavior observed for these two formulations must be linked to the threefold difference in content of the aerolization excipient L-LC. The presence of large particles was reflected in the ACI size distribution profile of RH-loaded microparticles. The technique-dependent variability in observed mean particle size is well documented: laser diffraction measurements give appreciably longer mean diameters than impaction studies due to the effects on aerosolization performance of slip, shape and density.[51,52] The density of microparticles studied by impaction appears to have been affected by the incorporation of RH. This is reflected by the lower MMAD values relative to the corresponding geometric diameters determined for BD formulations. It is possible that aerolization performance also reflects changes in the shape of microparticles, which in turn are consequent to the differences in composition. Marked differences between MMAD values and geometric diameters were observed with all three formulations.

The behavior of microparticles in artificial mucus. Dispersion in the mucin medium effected a reduction in the surface charge of empty formulations. The influence of the mucoadhesive content CS to the ζ-potential of the system is illustrated in Figure 5A. Indicative of the strong association of particles with mucin, the surface charge of S3 was seen to be reduced from 37.5 mV to 8.8 mV while those for S6 and S4 were correspondingly reduced to 9.8 mV and at 10.2

mV. For comparison, the mucin medium is characterized by a surface charge of -18.6±1.45 mV. Consistent with the strong association of mucin with MCs is the observed unimodal distribution profiles characterizing the ζ-potential measurements (Supplementary Information Figure S3).

In accord with their limited impact on the integrity of the mucus layer, the fluorescently modified formulations penetrated the artificial mucus layer to a limited extent, Figure 5B, with RH1 and RH3 presenting values of 3.25% and 2.21% penetration, respectively; these differences are statistically significant at the $p<0.05$ level. Notably, of these two formulations, it is RH1 (the formulation with the higher DPPC content; DPPC is a natural component of mucus) that displays a higher propensity for the mucin network. The influence of CS is exemplified by the behavior of RH2, which was characterized by a corresponding value of 5.34% ($p<0.05$).

Penetration through mucus was followed visually over a 24 h period (Figure 5C). Large amounts of RH1 and RH2 were seen to penetrate the artificial mucus layer and deposit onto the gelatin surface. For the RH3 formulation, the number of particles approaching the gelatin surface was seen to be limited by the observed rate of penetration through mucus.

The behavior of BD microparticles in homogenised mucus. The mucoadhesion performance of budesonide-loaded MCs was studied further with the aid of a texture analyzer. In an experiment designed to assess the mucoadhesive behavior of BD formulations, a physiologically relevant amount of each of BD1, BD2 and BD3 was mixed with a specified amount of homogenized mucus. A specified amount of each mixture (0.25 mL) was placed onto a glass slide with the aid of an automatic pipette. Each glass slide was placed on the TA stand. The TA probe was set to exert a force of 5g and lowered into the probed sample. After 10 seconds the probe was raised and the detachment profile was recorded. For control experiments, homogenised mucus was replaced by distilled water. A comparative assessment of the profiles

characterizing each of the BD formulations showed that all formulations were similarly mucoadhesive and also identified BD2 as that associated with slightly stronger mucoadhesive interactions (as quantified by the area under the mucoadhesion curve; work of adhesion) and also the desirable property of instantaneous (<<2 sec) onset of mucoadhesive behavior (Supplementary Information, Figure S4).

To assess the effect of contact time between the BD solids and mucus, a sample of each type of microparticle was placed onto one side of double-sided adhesive tape, the other side of which was attached to the flat end of the probe (Supplementary Information, Figure S5), and the probe (set at a force of 5g) was again lowered into the homogenised mucus (0.25mL) and allowed to interact for a specified time (10 sec) such that the microparticles become integrated into the test medium) before the raising of the probe; microparticles-free homogenised mucus provided the control. Data for the 10 sec experiment, presented as Supplementary Information (Figure S6), confirm the rapid integration of BD2 into the mucus layer. In accord with expectation on the basis of differences in surface energy, comparative data collected for the BD formulations in contact with homogenized mucus or with a distilled water control indicated the higher affinity of the formulations for mucus than for water, as is illustrated by the longer acting force of adhesion for BD2 against homogenized mucus as compared with that against distilled water. Comparison (Figure 6) of the shapes of the positive portions of the force *vs* time curve reveals the maximum forces exerted onto the probe by the water or mucus media are very similar (as demonstrated by the comparison of peak maxima) but, consistent with more cohesive nature of the mucus-microparticle system, the detachment of the probe from the mucus substrate occurs over a longer time period. Nonetheless, the data is semiquantitative (the results are presented as force *vs* time plots, since conversion into Work of Adhesion data is impeded by the ill-defined limits of the

integration) due to the small but significant variations in the number of particles initially held by the double-sided adhesive tape. The negative part of the same plot (Figure 6) is characterised by two distinct segments. Instantaneous adhesive interactions develop between the probe and either medium, but between time 0 and the onset of the 10 sec plateau (interaction time) there is a marked difference in behaviour: the pulling force (adhesion) exerted by water on initial contact with the microparticle-decorated probe is more pronounced than that exerted by mucus but after the 10 sec interaction time, the adhesive-interaction profiles become identical.

Since all BD formulations developed mucoadhesive interactions well within the 10 sec timescale, to provide an indication of the time-dependence of the mucoadhesive effect characterising each formulation, mixtures (0.5 ml) of each of the BD formulations and homogenised mucus were placed in separate vials of identical dimensions. (Parallel control samples utilised distilled water in the place of homogenised mucus.) The mucoadhesion profiles (force, 5g; probe contact time 10 sec) recorded at 5 min and at 30 min after mixing were identical, indicating that the mucus-mucoadhesive system was stable over this, therapeutically relevant, timescale.

***In vitro* release studies in SLF.** For all BD loaded MCs, the percentage loading of the drug was of the order of 4.9% w/w of the total mass of the formulation, which is in good agreement with the 5% w/w BD content in total solids incorporated in the feed solutions.

Drug release in SLF was monitored over 24 h, Figure 7. Similar release profiles were recorded for all formulations over the first 60 min, with approximately 40% of the incorporated drug seen to be released. Observations over 12 h revealed distinct differences in release profiles. Under the adopted experimental protocol, BD3 released *ca*. 90% of its therapeutic content within 4 h; and almost 100% within 6 h. Corresponding release rates for BD1 and BD2 were of the order of 80%

at 4 h and 90% at 6h. These statistically significant ($P<0.05$) differences are attributed to the relatively high content of the water soluble molecules PVA and LCS in the BD3 formulation, as compared with the BD1 and BD2 homologues. Symptomatic of the influence exerted by its high proportions of lipid content and low proportions of water soluble components, BD1 released its entire drug content at a rate that decelerated progressively over the 24 h monitoring time period of the experiment.

Cell viability studies. The data presented in Figure 8 (A, B & C) indicate that, over the 48 h timespan and at the <2 mg/mL concentration level, budesonide-loaded microparticles do not exert any noticeable adverse effect on the cellular proliferation of Calu-3 cultures. In parallel, no permanent effect on the integrity of the Calu-3 cells membrane was observed upon treatment with the microparticles under the same experimental conditions (Figure 8D).

CONCLUSIONS

A multicomponent microparticulate drug carrier has been developed, which is proposed to merit further investigation as vehicle for the efficient delivery of the corticosteroid budesonide to the respiratory tract. The microparticles were prepared at *ca*. 30% yield by means of a spray-drying process and formulations were engineered such that they exhibit good sphericity (mean particle size: 3.9-6.5 μm) and a surface charge in the range 29-51 mV. To meet the performance demands that are integral to effective pulmonary delivery, the formulations incorporate a lung surfactant (dipalmitoylphosphatidylcholine, 15-45% w/w) with materials that are known for their desirable effects on morphology (polyvinyl-alcohol, 15-40% w/w), aerosolization (L-leucine 3-9% w/w) and mucoadhesion (chitosan 2-6% w/w), and are further designed in a manner that allows the controlled release of a therapeutically active molecule (budesonide, 5% w/w).

Aerolization studies of the proposed microparticles indicated the promise of formulation BD3/RH3 (respective MMAD and FPF% values of 3.97μm and 65.16) as a means for the delivery of active compound to the lower respiratory tract. The suitability of the formulations for use in pulmonary therapy has been further indicated by evaluations employing two *in vitro* models of artificial mucosa to assess the effects of the mucus substrate on surface charge and to evaluate mucooadhesion and the mucosa-penetration profile. Mucoadhesion and mucus penetrating tests, identified formulation BD2/RH2 (MMAD, 5.64 μm; FPF, 38.28%) as that which merits further evaluation. The biocompatibility of the formulations has been indicated by studies that assessed the proliferation and integrity of Calu-3 cell monolayers.

Supporting Information

Figure S1. SEM micrograph of the typical morphology of distorted particles.

Figure S2. Deposition of RH-loaded MCs at the stages of ACI.

Figure S3. Typical ζ-potential measurement, showing unimodal distribution.

Figure S4. Comparative mucoadhesion profiles for BD1, BD2 and BD3 in mixute with mucus.

Figure S5. Schematic of the texture analyser probe showing the position of the test sample on the double-sided adhesive tape.

Figure S6. The mucoadhesion profiles of BD1, BD2 and BD3 as obtained by the adhesive-tape test.

Corresponding author

*Dr Dimitrios G. Fatouros, Laboratory of Pharmaceutical Technology, School of Pharmacy, Aristotle University of Thessaloniki GR, 54124 e-mail: dfatouro@pharm.auth.gr

Author Contributions

The manuscript was written through contributions of all authors. All authors have approved the final version of the manuscript.

Notes

The authors declare no competing financial interest.

ABBREVIATIONS

ACI, Andersen Cascade Impactor; BD, budesonide; CS, chitosan; DPPC, dipalmitoylphosphatidylcholine; DSC differential scanning calorimetry; FPF, fine particle fraction; FTIR, Fourier transform infrared spectroscopy; GSD, geometric standard deviation; HPLC, high performance liquid chromatography; L-LC, L-leucine; LCS, a-lactose monohydrate; MCs, multicomponent carriers; MMAD, mass mean aerodynamic diameter; PSD, particle size distribution; PVA, polyvinyl alcohol; RH, rhodamine b; SEM, scanning electron microscopy; SLF, simulated lung fluid;

REFERENCES

(1) Patton, J. S.; Byron, P. R. Inhaling Medicines: Delivering Drugs to the Body through the Lungs. *Nat. Rev. Drug Discov.* **2007**, *6* (1), 67–74.

(2) Zhou, Q. (Tony); Leung, S. S. Y.; Tang, P.; Parumasivam, T.; Loh, Z. H.; Chan, H.-K. Inhaled Formulations and Pulmonary Drug Delivery Systems for Respiratory Infections. *Adv. Drug Deliv. Rev.* **2015**, *85*, 83–99.

(3) Bosquillon, C.; Lombry, C.; Préat, V.; Vanbever, R. Influence of Formulation Excipients and Physical Characteristics of Inhalation Dry Powders on Their Aerosolization Performance. *J. Control. Release* **2001**, *70* (3), 329–339.

(4) Groneberg, D. A.; Witt, C.; Wagner, U.; Chung, K. F.; Fischer, A. Fundamentals of Pulmonary Drug Delivery. *Respir. Med.* **2003**, *97* (4), 382–387.

(5) Lai, S. K.; Wang, Y.-Y.; Hanes, J. Mucus-Penetrating Nanoparticles for Drug and Gene Delivery to Mucosal Tissues. *Adv. Drug Deliv. Rev.* **2009**, *61* (2), 158–171.

(6) Beach, E. R.; Tormoen, G. W.; Drelich, J.; Han, R. Pull-off Force Measurements between Rough Surfaces by Atomic Force Microscopy. *J. Colloid Interface Sci.* **2002**, *247* (1), 84–99.

(7) Kinnunen, H.; Hebbink, G.; Peters, H.; Huck, D.; Makein, L.; Price, R. Extrinsic Lactose Fines Improve Dry Powder Inhaler Formulation Performance of a Cohesive Batch of Budesonide via Agglomerate Formation and Consequential Co-Deposition. *Int. J. Pharm.* **2015**, *478* (1), 53–59.

(8) Ourique, A. F.; Chaves, P. dos S.; Souto, G. D.; Pohlmann, A. R.; Guterres, S. S.; Beck, R. C. R. Redispersible Liposomal-N-Acetylcysteine Powder for Pulmonary Administration: Development, in Vitro Characterization and Antioxidant Activity. *Eur. J. Pharm. Sci.* **2014**, *65*, 174–182.

(9) Li, M.; Zhang, T.; Zhu, L.; Wang, R.; Jin, Y. Liposomal Andrographolide Dry Powder Inhalers for Treatment of Bacterial Pneumonia via Anti-Inflammatory Pathway. *Int. J. Pharm.* **2017**, *528* (1–2), 163–171.

(10) Takeuchi, I.; Tetsuka, Y.; Nii, T.; Shinogase, M.; Makino, K. Inhalable Nanocomposite Particles Using Amino Acids with Improved Drug Content and Humidity Resistance.

Colloids Surfaces A Physicochem. Eng. Asp. **2017**, *529*, 387–393.

(11) Yu, J.; Chan, H.-K.; Gengenbach, T.; Denman, J. A. Protection of Hydrophobic Amino Acids against Moisture-Induced Deterioration in the Aerosolization Performance of Highly Hygroscopic Spray-Dried Powders. *Eur. J. Pharm. Biopharm.* **2017**, *119*, 224–234.

(12) Debnath, S. K.; Saisivam, S.; Omri, A. PLGA Ethionamide Nanoparticles for Pulmonary Delivery: Development and in Vivo Evaluation of Dry Powder Inhaler. *J. Pharm. Biomed. Anal.* **2017**, *145*, 854–859.

(13) Kolte, A.; Patil, S.; Lesimple, P.; Hanrahan, J. W.; Misra, A. PEGylated Composite Nanoparticles of PLGA and Polyethylenimine for Safe and Efficient Delivery of pDNA to Lungs. *Int. J. Pharm.* **2017**, *524* (1–2), 382–396.

(14) Loira-Pastoriza, C.; Todoroff, J.; Vanbever, R. Delivery Strategies for Sustained Drug Release in the Lungs. *Adv. Drug Deliv. Rev.* **2014**, *75*, 81–91.

(15) Pilcer, G.; Wauthoz, N.; Amighi, K. Lactose Characteristics and the Generation of the Aerosol. *Adv. Drug Deliv. Rev.* **2012**, *64* (3), 233–256.

(16) Vanbever, R.; Mintzes, J. D.; Wang, J.; Nice, J.; Chen, D.; Batycky, R.; Langer, R.; Edwards, D. A. Formulation and Physical Characterization of Large Porous Particles for Inhalation. *Pharm. Res.* **1999**, *16* (11), 1735–1742.

(17) Sham, J. O.-H.; Zhang, Y.; Finlay, W. H.; Roa, W. H.; Löbenberg, R. Formulation and Characterization of Spray-Dried Powders Containing Nanoparticles for Aerosol Delivery to the Lung. *Int. J. Pharm.* **2004**, *269* (2), 457–467.

(18) Vehring, R. Pharmaceutical Particle Engineering via Spray Drying. *Pharm. Res.* **2008**, *25* (5), 999–1022.

(19) Sou, T.; Kaminskas, L. M.; Nguyen, T.-H.; Carlberg, R.; McIntosh, M. P.; Morton, D. A. V. The Effect of Amino Acid Excipients on Morphology and Solid-State Properties of Multi-Component Spray-Dried Formulations for Pulmonary Delivery of Biomacromolecules. *Eur. J. Pharm. Biopharm.* **2013**, *83* (2), 234–243.

(20) Hoe, S.; Ivey, J. W.; Boraey, M. A.; Shamsaddini-Shahrbabak, A.; Javaheri, E.; Matinkhoo, S.; Finlay, W. H.; Vehring, R. Use of a Fundamental Approach to Spray-Drying Formulation Design to Facilitate the Development of Multi-Component Dry Powder Aerosols for Respiratory Drug Delivery. *Pharm. Res.* **2014**, *31* (2), 449–465.

(21) Sou, T.; Forbes, R. T.; Gray, J.; Prankerd, R. J.; Kaminskas, L. M.; McIntosh, M. P.; Morton, D. A. V. Designing a Multi-Component Spray-Dried Formulation Platform for Pulmonary Delivery of Biopharmaceuticals: The Use of Polyol, Disaccharide, Polysaccharide and Synthetic Polymer to Modify Solid-State Properties for Glassy Stabilisation. *Powder Technol.* **2016**, *287*, 248–255.

(22) Yang, Y.; Cheow, W. S.; Hadinoto, K. Dry Powder Inhaler Formulation of Lipid–polymer Hybrid Nanoparticles via Electrostatically-Driven Nanoparticle Assembly onto Microscale Carrier Particles. *Int. J. Pharm.* **2012**, *434* (1–2), 49–58.

(23) Salama, R.; Hoe, S.; Chan, H.-K.; Traini, D.; Young, P. M. Preparation and Characterisation of Controlled Release Co-Spray Dried Drug–polymer Microparticles for Inhalation 1: Influence of Polymer Concentration on Physical and in Vitro Characteristics. *Eur. J. Pharm. Biopharm.* **2008**, *69* (2), 486–495.

(24) Salama, R. O.; Traini, D.; Chan, H.-K.; Sung, A.; Ammit, A. J.; Young, P. M. Preparation and Evaluation of Controlled Release Microparticles for Respiratory Protein Therapy. *J. Pharm. Sci.* **2009**, *98* (8), 2709–2717.

(25) Karimi, K.; Katona, G.; Csóka, I.; Ambrus, R. Physicochemical Stability and Aerosolization Performance of Dry Powder Inhalation System Containing Ciprofloxacin Hydrochloride. *J. Pharm. Biomed. Anal.* **2018**, *148*, 73–79.

(26) Veldhuizen, R.; Nag, K.; Orgeig, S.; Possmayer, F. The Role of Lipids in Pulmonary Surfactant. *Biochim. Biophys. Acta - Mol. Basis Dis.* **1998**, *1408* (2–3), 90–108.

(27) Cook, R. O.; Pannu, R. K.; Kellaway, I. W. Novel Sustained Release Microspheres for Pulmonary Drug Delivery. *J. Control. Release* **2005**, *104* (1), 79–90.

(28) Mansour, H.; Duan; Vogt; Li; Hayes, Jr., D. Design, Characterization, and Aerosolization of Organic Solution Advanced Spray-Dried Moxifloxacin and Ofloxacin Dipalmitoylphosphatidylcholine (DPPC) Microparticulate/nanoparticulate Powders for Pulmonary Inhalation Aerosol Delivery. *Int. J. Nanomedicine* **2013**, 3489.

(29) Meenach, S. A.; Anderson, K. W.; Hilt, J. Z.; McGarry, R. C.; Mansour, H. M. High-Performing Dry Powder Inhalers of Paclitaxel DPPC/DPPG Lung Surfactant-Mimic Multifunctional Particles in Lung Cancer: Physicochemical Characterization, In Vitro Aerosol Dispersion, and Cellular Studies. *AAPS PharmSciTech* **2014**, *15* (6), 1574–1587.

(30) Li, L.; Sun, S.; Parumasivam, T.; Denman, J. A.; Gengenbach, T.; Tang, P.; Mao, S.; Chan, H.-K. L -Leucine as an Excipient against Moisture on in Vitro Aerosolization Performances of Highly Hygroscopic Spray-Dried Powders. *Eur. J. Pharm. Biopharm.* **2016**, *102*, 132–141.

(31) Boraey, M. A.; Hoe, S.; Sharif, H.; Miller, D. P.; Lechuga-Ballesteros, D.; Vehring, R. Improvement of the Dispersibility of Spray-Dried Budesonide Powders Using Leucine in an Ethanol–water Cosolvent System. *Powder Technol.* **2013**, *236*, 171–178.

(32) Williams III, R. O.; Barron, M. K.; José Alonso, M.; Remuñán-López, C. Investigation of

a pMDI System Containing Chitosan Microspheres and P134a. *Int. J. Pharm.* **1998**, *174* (1–2), 209–222.

(33) Karavasili, C.; Katsamenis, O. L.; Bouropoulos, N.; Nazar, H.; Thurner, P. J.; van der Merwe, S. M.; Fatouros, D. G. Preparation and Characterization of Bioadhesive Microparticles Comprised of Low Degree of Quaternization Trimethylated Chitosan for Nasal Administration: Effect of Concentration and Molecular Weight. *Langmuir* **2014**, *30* (41), 12337–12344.

(34) Yamamoto, H.; Kuno, Y.; Sugimoto, S.; Takeuchi, H.; Kawashima, Y. Surface-Modified PLGA Nanosphere with Chitosan Improved Pulmonary Delivery of Calcitonin by Mucoadhesion and Opening of the Intercellular Tight Junctions. *J. Control. Release* **2005**, *102* (2), 373–381.

(35) Al-Qadi, S.; Grenha, A.; Carrión-Recio, D.; Seijo, B.; Remuñán-López, C. Microencapsulated Chitosan Nanoparticles for Pulmonary Protein Delivery: In Vivo Evaluation of Insulin-Loaded Formulations. *J. Control. Release* **2012**, *157* (3), 383–390.

(36) Humphrey, S. P.; Williamson, R. T. A Review of Saliva: Normal Composition, Flow, and Function. *J. Prosthet. Dent.* **2001**, *85* (2), 162–169.

(37) Yaws, C. L. *Yaws' Thermophysical Properties of Chemicals and Hydrocarbons (Electronic Edition)*; 2010.

(38) Ungaro, F.; D'Angelo, I.; Coletta, C.; d'Emmanuele di Villa Bianca, R.; Sorrentino, R.; Perfetto, B.; Tufano, M. A.; Miro, A.; La Rotonda, M. I.; Quaglia, F. Dry Powders Based on PLGA Nanoparticles for Pulmonary Delivery of Antibiotics: Modulation of Encapsulation Efficiency, Release Rate and Lung Deposition Pattern by Hydrophilic Polymers. *J. Control. Release* **2012**, *157* (1), 149–159.

(39) Moss, O. R. Simulants of Lung Interstitial Fluid. *Health Phys.* **1979**, *36* (3), 447–448.

(40) Ungaro, F.; d'Emmanuele di Villa Bianca, R.; Giovino, C.; Miro, A.; Sorrentino, R.; Quaglia, F.; La Rotonda, M. I. Insulin-Loaded PLGA/cyclodextrin Large Porous Particles with Improved Aerosolization Properties: In Vivo Deposition and Hypoglycaemic Activity after Delivery to Rat Lungs. *J. Control. Release* **2009**, *135* (1), 25–34.

(41) Nolan, L. M.; Tajber, L.; McDonald, B. F.; Barham, A. S.; Corrigan, O. I.; Healy, A. M. Excipient-Free Nanoporous Microparticles of Budesonide for Pulmonary Delivery. *Eur. J. Pharm. Sci.* **2009**, *37* (5), 593–602.

(42) Vizirianakis, I. S.; Tsiftsoglou, A. S. N6-Methyladenosine Inhibits Murine Erythroleukemia Cell Maturation by Blocking Methylation of RNA and Memory via Conversion to S-(N6-Methyl)-Adenosylhomocysteine. *Biochem. Pharmacol.* **1995**, *50* (11), 1807–1814.

(43) Mu, L.; Feng, S. . Fabrication, Characterization and in Vitro Release of Paclitaxel (Taxol®) Loaded Poly (Lactic-Co-Glycolic Acid) Microspheres Prepared by Spray Drying Technique with Lipid/cholesterol Emulsifiers. *J. Control. Release* **2001**, *76* (3), 239–254.

(44) Vila, A.; Sánchez, A.; Tobío, M.; Calvo, P.; Alonso, M. J. Design of Biodegradable Particles for Protein Delivery. *J. Control. Release* **2002**, *78* (1–3), 15–24.

(45) Kundu, S.; Matsuoka, H.; Seto, H. Zwitterionic Lipid (DPPC)–protein (BSA) Complexes at the Air–water Interface. *Colloids Surfaces B Biointerfaces* **2012**, *93*, 215–218.

(46) Bruni, G.; Maggi, L.; Tammaro, L.; Canobbio, A.; Di Lorenzo, R.; D'aniello, S.; Domenighini, C.; Berbenni, V.; Milanese, C.; Marini, A. Fabrication, Physico-Chemical, and Pharmaceutical Characterization of Budesonide-Loaded Electrospun Fibers for Drug

Targeting to the Colon. *J. Pharm. Sci.* **2015**, *104* (11), 3798–3803.

(47) Ali, H. R. H.; Edwards, H. G. M.; Kendrick, J.; Munshi, T.; Scowen, I. J. Vibrational Spectroscopic Study of Budesonide. *J. Raman Spectrosc.* **2007**, *38* (7), 903–908.

(48) Arrondo, J. L.; Goñi, F. M. Infrared Studies of Protein-Induced Perturbation of Lipids in Lipoproteins and Membranes. *Chem. Phys. Lipids* **1998**, *96* (1–2), 53–68.

(49) Corrigan, D. O.; Healy, A. M.; Corrigan, O. I. The Effect of Spray Drying Solutions of Polyethylene Glycol (PEG) and lactose/PEG on Their Physicochemical Properties. *Int. J. Pharm.* **2002**, *235* (1–2), 193–205.

(50) Raula, J.; Lahde, A.; Kauppinen, E. Aerosolization Behavior of Carrier-Free L-Leucine Coated Salbutamol Sulphate Powders. *Int. J. Pharm.* **2009**, *365* (1–2), 18–25.

(51) Chougule, M.; Padhi, B.; Misra, A. Development of Spray Dried Liposomal Dry Powder Inhaler of Dapsone. *AAPS PharmSciTech* **2008**, *9* (1), 47–53.

(52) Pilcer, G.; Vanderbist, F.; Amighi, K. Correlations between Cascade Impactor Analysis and Laser Diffraction Techniques for the Determination of the Particle Size of Aerosolised Powder Formulations. *Int. J. Pharm.* **2008**, *358* (1–2), 75–81.

TABLES

Table 1. Composition, process yield and ζ-potential values of empty formulations.

	Excipient content %w/w					Solvent	Process Yield	ζ-potential
ID	PVA	CS	L-LC	DPPC	LCS	H_2O:EtOH	%	mV
S1	15	2	3	45	35		20.7 ± 2.7	29.3 ± 1.7
S2	30	2	3	20	45		28.1 ± 1.4	40.8 ± 0.9
S3	40	2	3	15	40	30:70	30.3 ± 0.9	37.5 ± 1.6
S4	35	6	9	15	35		29.7 ± 0.8	51.4 ± 0.3
S5	30	2	3	30	35		28.9 ± 1.8	29.7 ± 1.5
S6	30	2	3	30	35	15:85	32.1 ± 1.5	32.3 ± 2.4
S7	40	2	3	15	40		31.3 ± 1.2	33.8 ± 1.3

Table 2. Composition and process yield of budesonide- or Rhodamine B-loaded formulations.

	Excipient content %w/w							Process Yield
ID	PVA	CS	L-LC	DPPC	LCS	BD	RH	%
BD1	30	2	3	30	30	5	-	33.8 ± 1.1
BD2	35	6	9	15	30	5	-	30.4 ± 1.8
BD3	40	2	3	15	35	5	-	29.2 ± 1.6
RH1	30	2	3	30	30	3	2	34.6 ± 1.9
RH2	35	6	9	15	30	3	2	31.1 ± 1.3
RH3	40	2	3	15	35	3	2	31.9 ± 1.5

Table 3. Size distribution parameters of budesonide and Rhodamine B-loaded formulations.

	Spraytec Particle Analysis			Andersen Cascade Impactor		
Formulation	$D_v(50)$ µm	Span	particles<5µm %	MMAD µm	GSD	FPF%
BD1/RH1	9.74 ± 0.29	2.75 ± 0.10	20.46 ± 0.55	6.51 ± 0.15	1.32 ± 0.17	22.67 ± 1.28
BD2/RH2	9.29 ± 0.18	2.48 ± 0.08	21.96 ± 0.44	5.64 ±0.21	1.2 ± 0.19	38.28 ± 2.01
BD3/RH3	8.98 ± 0.22	2.30 ± 0.07	23.57 ± 0.47	3.97 ± 0.24	2.5 ± 0.21	65.16 ± 2.34

FIGURE LEGENDS

FIGURE 1: SEM micrographs of empty (**A, B**, **C**) and drug loaded (**D**, **E**, **F**) formulations. A:S3, B:S4, C:S6, D:BD1, E:BD2, F:BD3.

FIGURE 2: FTIR spectra of loaded formulations and of their components.

FIGURE 3: DSC thermograms of (**A**) pure components and (**B**) empty and drug loaded formulations.

FIGURE 4: Size distribution of (**A**) BD1, (**B**) BD2, and (**C**) BD3 formulations, as obtained by Spraytec analysis software; and, (**D**) deposition of RH-loaded particles at the stages of the Andersen cascade impactor.

FIGURE 5: (**A**) The effect of mucin medium on the ζ-potentials of the carriers. (**B**) Permeation studies of Rhodamine B-loaded formulations on artificial mucus. (**C**) Illustration of the penetration procedure through artificial mucus, observed visually after 24 h of exposure.

FIGURE 6: The interaction of BD2 with homogenized mucus and with the distilled water control (tape test; 10 second contact time)

FIGURE 7: Release profiles of BD-loaded formulations on simulated lung fluid.

FIGURE 8: Calu-3 cell viability as assessed by the trypan blue assay following incubation with polymer-lipid microparticles at specified concentrations in the range 0.1-2 mg/mL. (**A**) BD1 microparticles, (**B**) BD2 microparticles, (**C**) BD3 microparticles, and (**D**) TEER values after cell exposure to 0.1 and 1 mg/mL at 4 h and at 8 h.

FIGURE 1

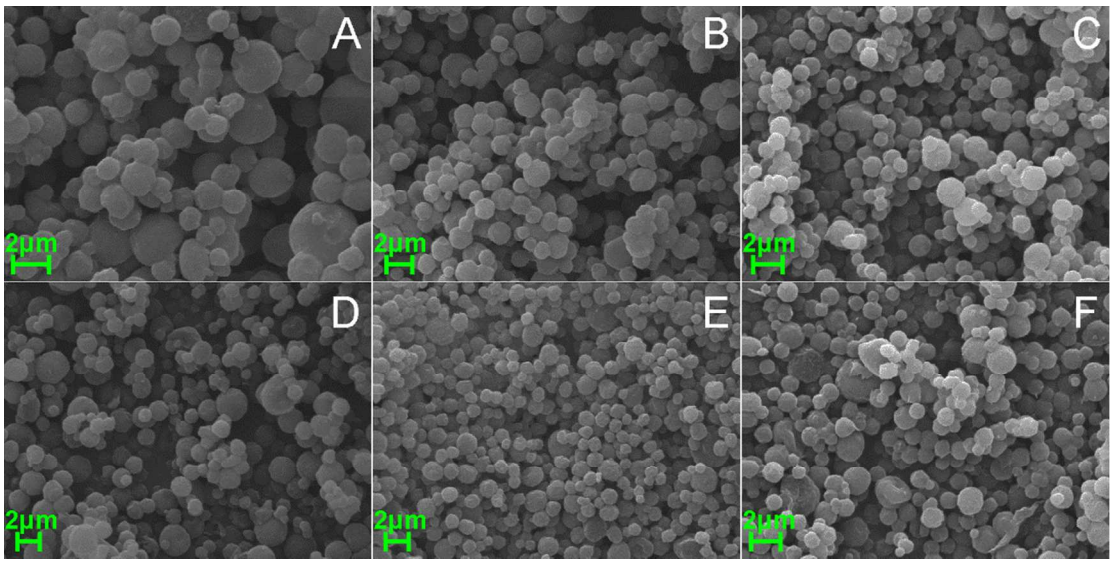

FIGURE 2

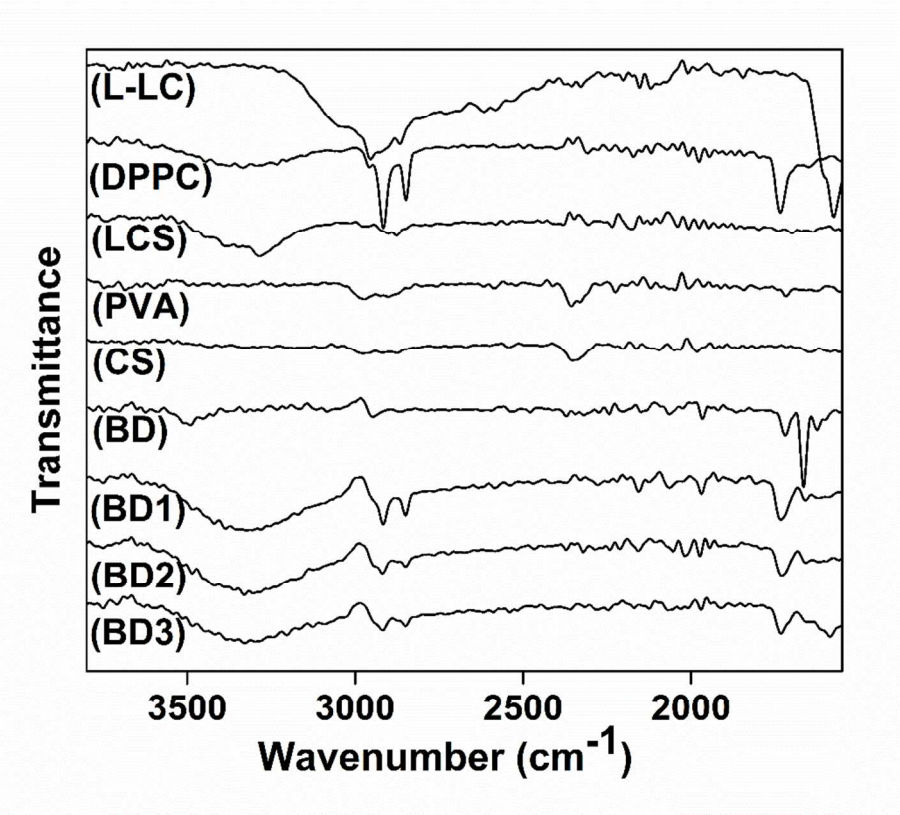
(L-LC)
(DPPC)
(LCS)
(PVA)
(CS)
(BD)
(BD1)
(BD2)
(BD3)
Transmittance
3500
3000
2500
2000
Wavenumber (cm-1)

FIGURE 3

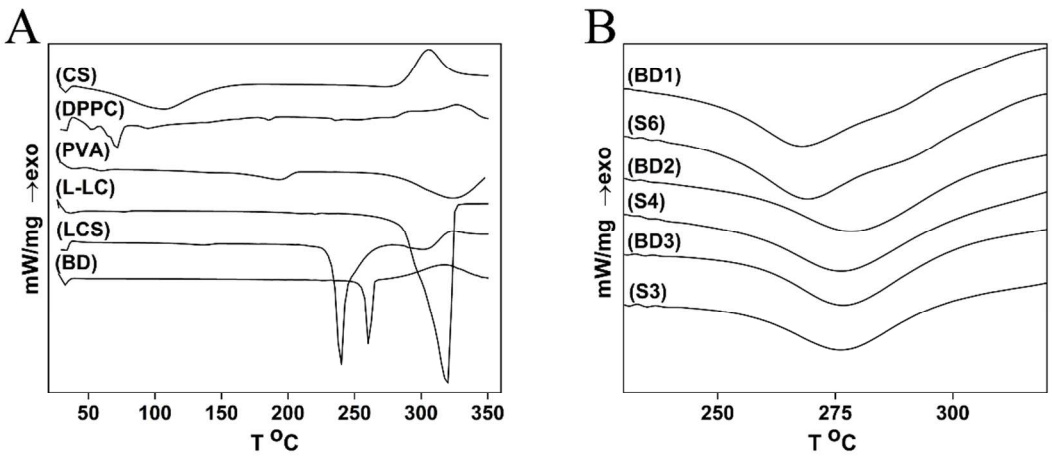
A
(CS)
(DPPC)
(PVA)
(L-LC)
(LCS)
(BD)
mW/mg →exo
50
100
150
200
250
300
350
T °C
B
(BD1)
(S6)
(BD2)
(S4)
(BD3)
(S3)
mW/mg →exo
250
275
300
T °C

FIGURE 4

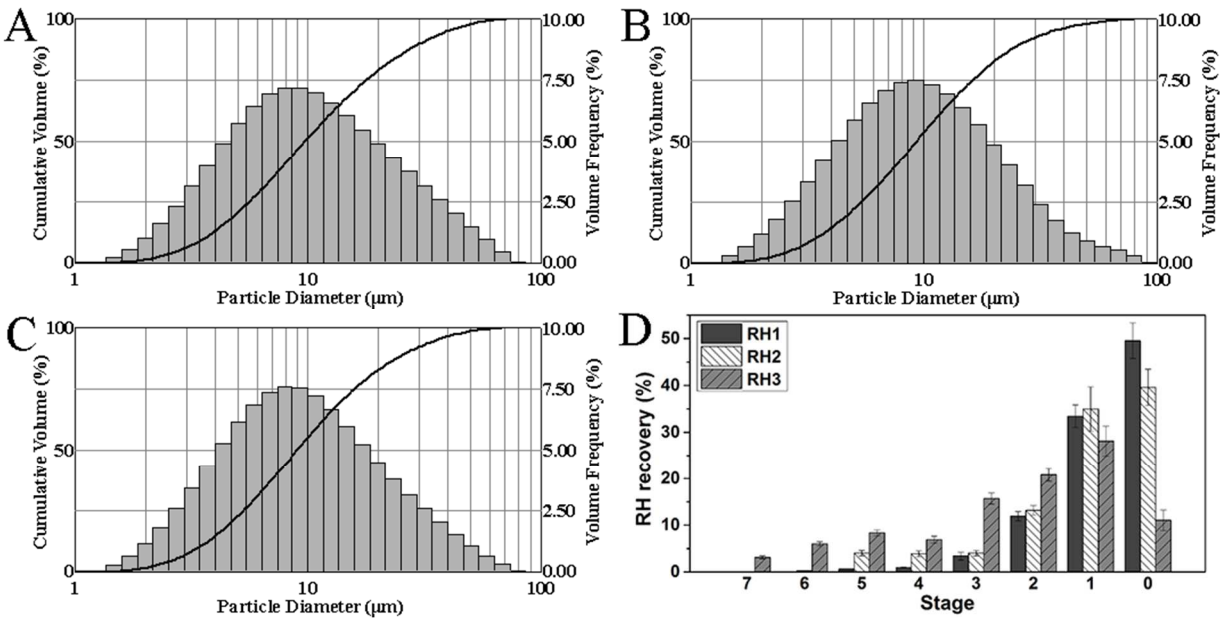
A
B
C
D
Cumulative Volume (%)
Volume Frequency (%)
Particle Diameter (μm)
RH1
RH2
RH3
RH recovery (%)
Stage

FIGURE 5

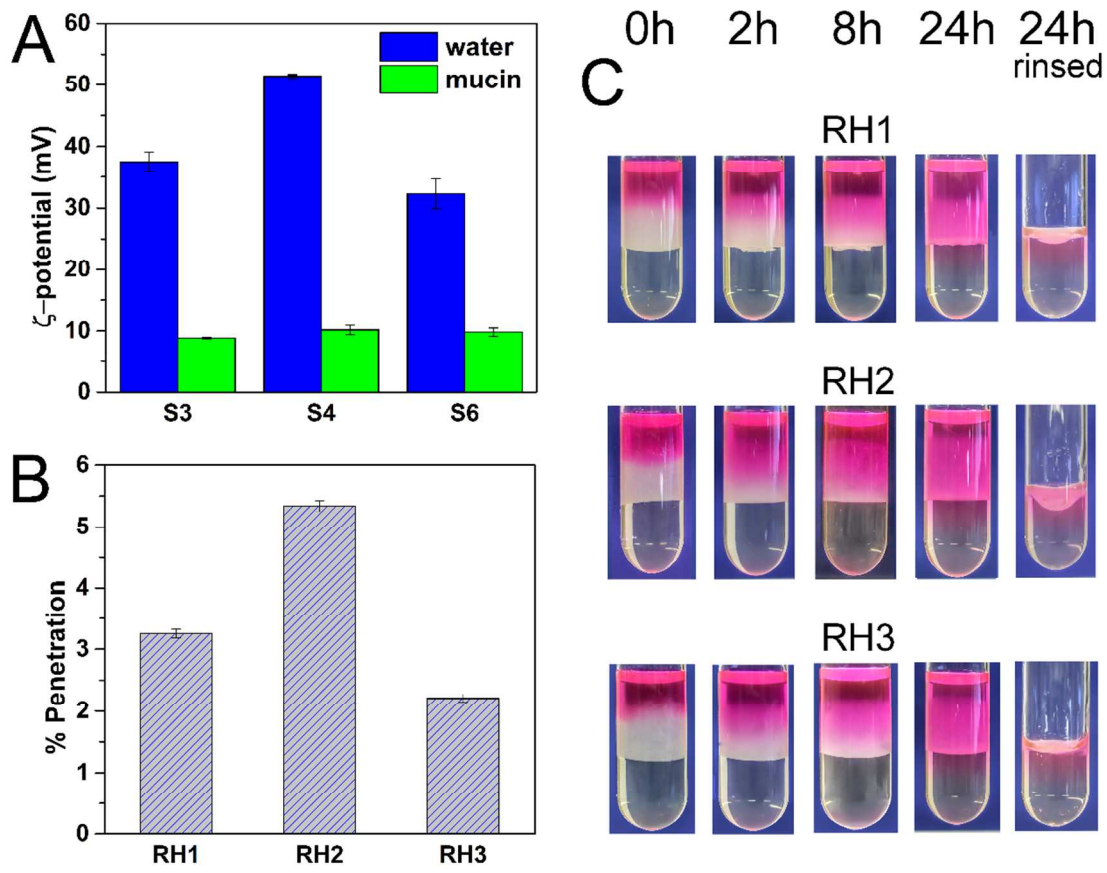
A
water
mucin
ζ–potential (mV)
0
10
20
30
40
50
60
S3
S4
S6
B
% Penetration
0
1
2
3
4
5
6
RH1
RH2
RH3
C
0h
2h
8h
24h
24h
rinsed
RH1
RH2
RH3

FIGURE 6

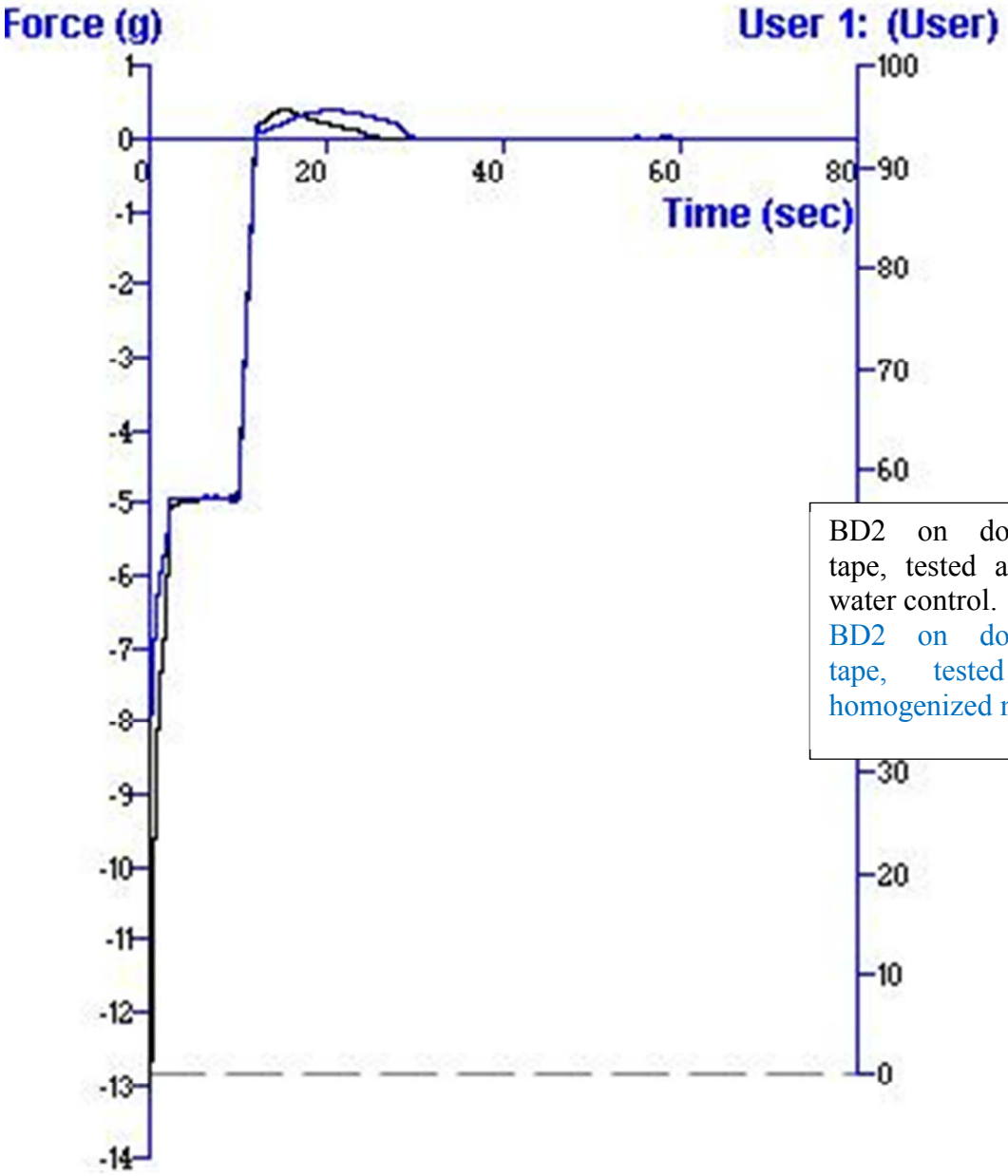
Force (g)
User 1: (User)
Time (sec)
1
0
-1
-2
-3
-4
-5
-6
-7
-8
-9
-10
-11
-12
-13
-14
0
20
40
60
80
100
90
80
70
60
30
20
10
0
BD2 on double-sided tape, tested against the water control.
BD2 on double-sided tape, tested against homogenized mucus.

FIGURE 7

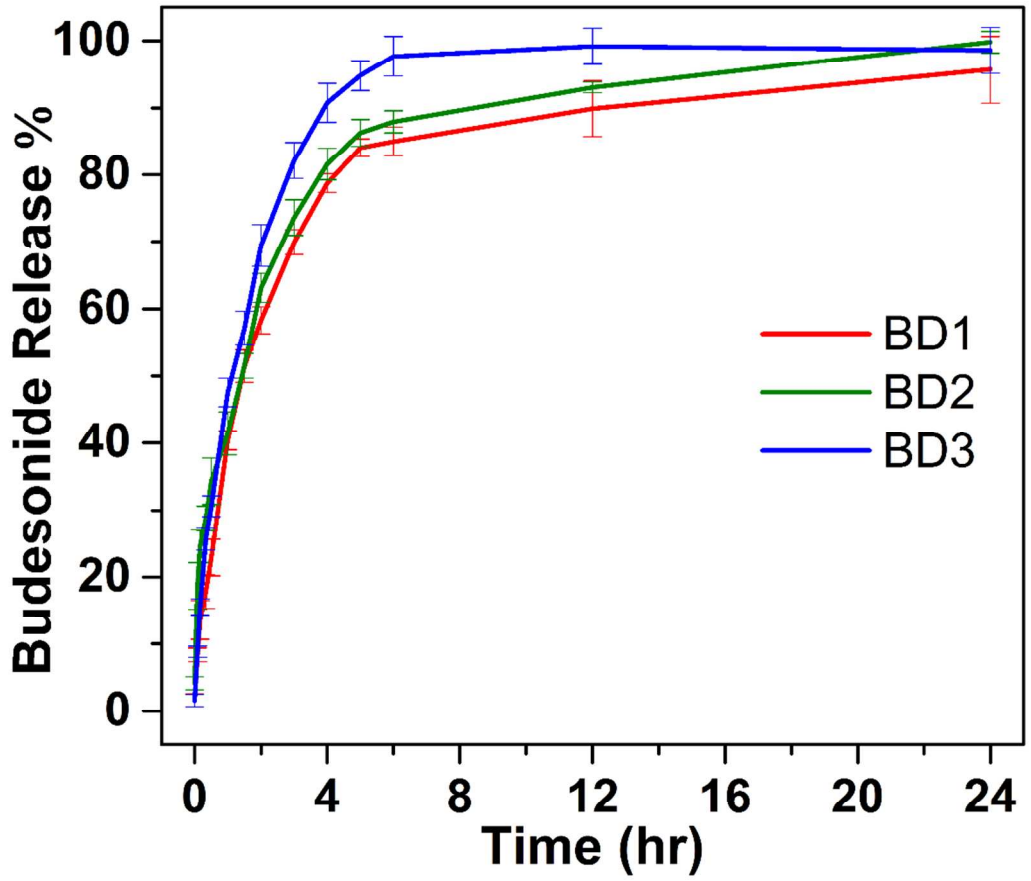
Budesonide Release %
100
80
60
40
20
0
0
4
8
12
16
20
24
Time (hr)
BD1
BD2
BD3

FIGURE 8

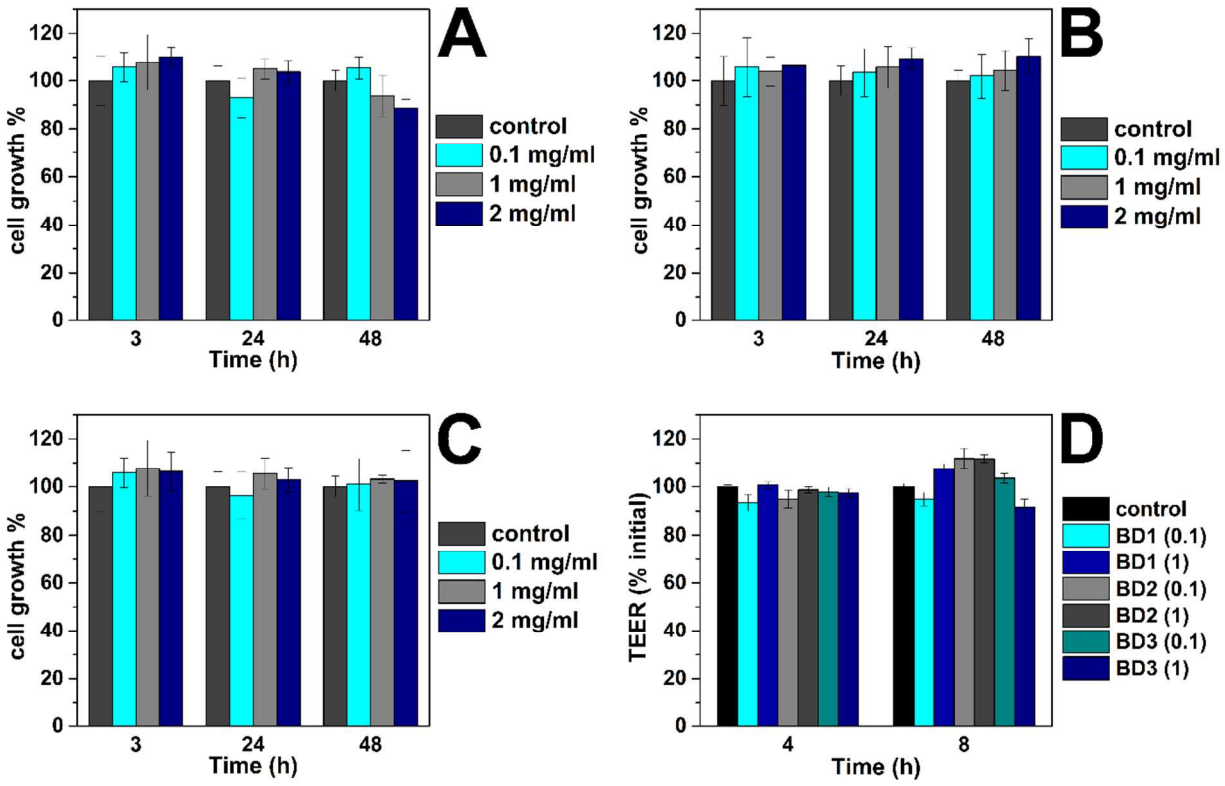
A
cell growth %
Time (h)
control
0.1 mg/ml
1 mg/ml
2 mg/ml
B
cell growth %
Time (h)
control
0.1 mg/ml
1 mg/ml
2 mg/ml
C
cell growth %
Time (h)
control
0.1 mg/ml
1 mg/ml
2 mg/ml
D
TEER (% initial)
Time (h)
control
BD1 (0.1)
BD1 (1)
BD2 (0.1)
BD2 (1)
BD3 (0.1)
BD3 (1)

TOC

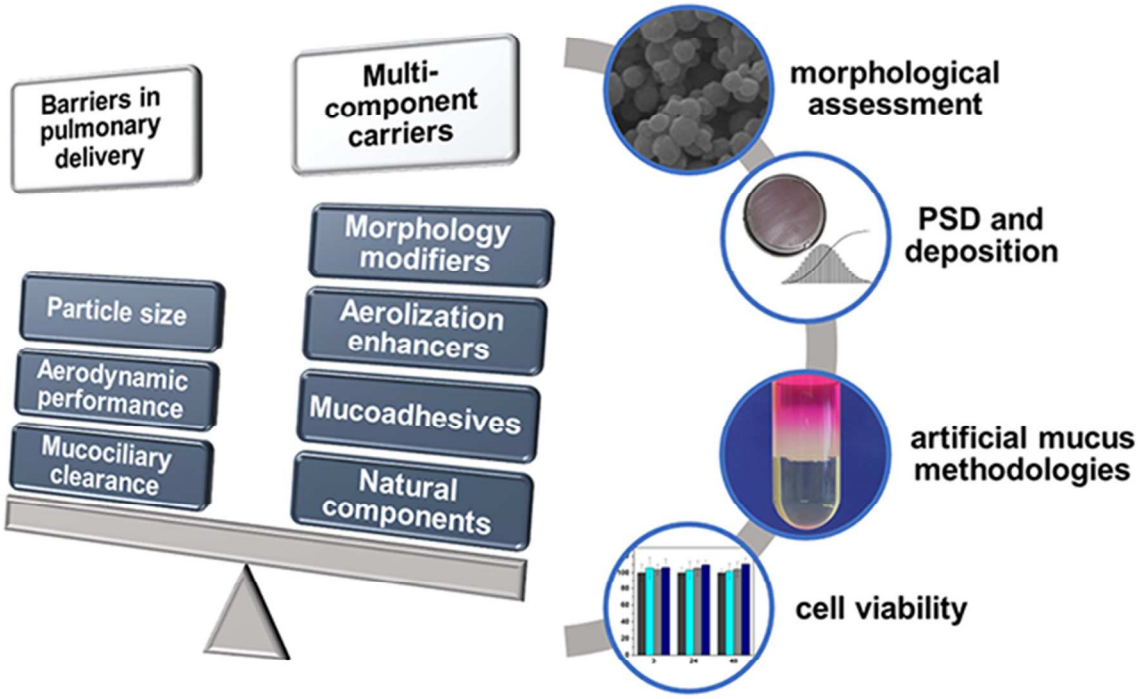
Barriers in pulmonary delivery
Multi-component carriers
Particle size
Aerodynamic performance
Mucociliary clearance
Morphology modifiers
Aerolization enhancers
Mucoadhesives
Natural components
morphological assessment
PSD and deposition
artificial mucus methodologies
cell viability